Seismic images of the sliver strike-slip fault and back thrust in the Andaman-Nicobar region

Satish C. Singh, Raphaele Moeremans, Jo Mcardle, Kjell Johansen

Seismic images of the sliver strike-slip fault and back thrust in the Andaman-Nicobar region

Satish C. Singh,[1] Raphaele Moeremans,[1] Jo McArdle,[2] and Kjell Johansen[2]

[1]   The sliver strike-slip Great Sumatra Fault (GSF) traverses mainland Sumatra from the Sunda Strait in the southeast to Banda Aceh in the northwest, and defines the present day plate boundary between the Sunda Plate in the north and the Burmese Sliver Plate in the south. It has been well studied on mainland Sumatra but poorly north of Banda Aceh in the Andaman Sea. Here we present deep seismic reflection images along the northward extension of the GSF over 700 km until it joins the Andaman Sea Spreading Centre, and we interpret these images in the light of earthquake, gravity, and bathymetry data. We find that the GSF has two strands between Banda Aceh and Nicobar Island: a transpression in the south and a deep narrow active rift system in the north, dotted with volcanoes in the center, suggesting that the volcanic arc is coincident with rifting. Farther north of Nicobar Island, an active strike-slip fault, the Andaman-Nicobar Fault, cuts through a rifted deep basin until its intersection with the Andaman Sea Spreading Centre. The volcanic arc lies just east of the rift basin. The western margin of this basin seems to be a rifted continental margin, tilted westward, and flooring the Andaman-Nicobar fore-arc basin. The Andaman-Nicobar fore-arc basin is bounded in the west by back thrusts similar to the West Andaman and Mentawai faults. The cluster of seismicity after the 2004 great Andaman-Sumatra earthquake just north of Nicobar Island coincides with the intersection of two strike-slip fault systems.

Citation: Singh, S. C., R. Moeremans, J. McArdle, and K. Johansen (2013), Seismic images of the sliver strike-slip fault and back thrust in the Andaman-Nicobar region, *J. Geophys. Res. Solid Earth*, *118*, 5208–5224, doi:10.1002/jgrb.50378.

1.   Introduction

[2]   The Andaman-Sumatra subduction system is a classic example of oblique subduction where the Indo-Australian oceanic plate subducts beneath the Eurasian plate, leading to slip partitioning into a trench-normal thrust component along the plate interface and a trench-subparallel strike-slip component accommodated by a sliver fault [*Fitch*, 1972; *McCaffrey*, 1992; 2009; *Curray*, 2005]. On mainland Sumatra, the strike-slip component is taken up along the Great Sumatran Fault (Figure 1). Nearly 1900 km long, the Great Sumatran Fault (GSF) stretches along the entire length of Sumatra Island, from the Sunda Strait in the southeast to Banda Aceh in the northwest [*Sieh and Natawidjaja*, 2000], mimicking the trend of the Sunda plate margin and finally joins a series of strike-slip faults in the Andaman Sea. Near Banda Aceh at the NW extremity, the GSF bifurcates into two strands: the Aceh Fault and the Seulimeum Fault (SF) that continue offshore north of Sumatra (Figures 1 and 2) toward Nicobar Island up to 7°N. Between 7°N and 11°N, the sliver

strike-slip motion is taken along the northward extension of the West Andaman Fault (WAF) [*Curray et al.*, 1979; *Curray*, 2005; *Cochran*, 2010], which we here name as the Andaman-Nicobar Fault (ANF). Farther north, the ANF is connected with the Sagaing Fault in Myanmar through a series of spreading centers and transform faults [*Kamesh Raju et al.*, 2004]. Around 7°N, the NNE-trending WAF, GSF, and ANF interact, but the precise nature of this interaction remains poorly constrained.

[3]   In the northwest of northern Sumatra, the WAF borders the fore arc Aceh Basin and the fore arc high accretionary wedge. Earlier, it was proposed that the WAF was a strike-slip fault [*Singh*, 2005; *Seeber et al.*, 2007; *Cochran*, 2010], similar to the Mentawai fault farther south, near central and southern Sumatra [*Diament et al.*, 1992]. However, recent seismic studies indicate that the WAF and Mentawai faults are mainly back thrusts and bound the continental crust in the east with for-arc ridges in the west [*Chauhan et al.*, 2009; *Singh et al.*, 2010; 2011a; *Mukti et al.*, 2012]. The absence of any strike-slip earthquakes along these faults further supports the idea of back thrusting. However, it is possible that Mentawai-WAF might have been sliver strike-slip faults accommodating strike-slip motion prior to the formation of GSF, but we do not have concrete evidence as yet. Between the Nicobar and Andaman fore-arc region, two faults have been identified: the Eastern Margin Fault (EMF) and the Diligent Fault (DF) [*Curray et al.*, 1979; *Curray*, 2005, *Cochran*, 2010], but their precise nature and roles in active deformation remain unknown.

[1]Laboratoire de Geoscience Marine, Institut de Physique du Globe de Paris, Paris, France.
[2]Petroleum Geo-Services, Singapore, Singapore.

Corresponding author: S. C. Singh, Laboratoire de Geoscience Marine, Institut de Physique du Globe de Paris, 1 rue Jussieu, 75238 Paris CEDEX 05, France. (singh@ipgp.fr)
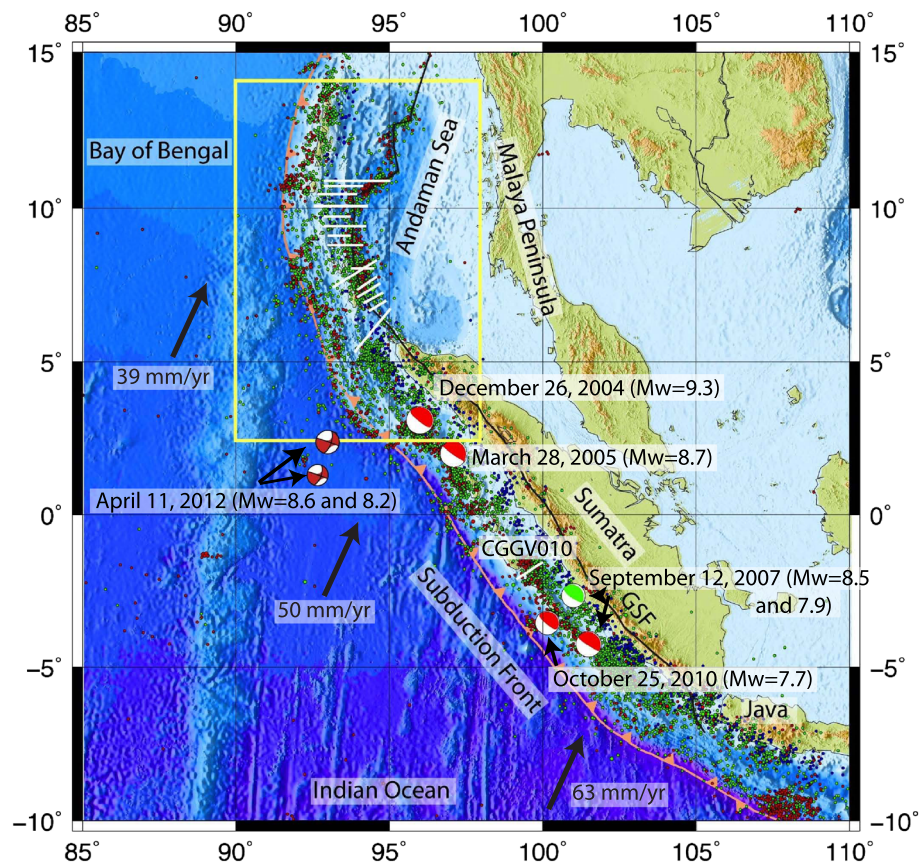
Figure 1. Map of the study area showing the Andaman-Sumatra Subduction zone and Andaman Sea Spreading Centre. Convergence directions and rates are shown with black arrows. Small circles represent earthquakes locations with hypocenter depth < 30 km (red), 30–60 km (green) and >60 km (blue). Focal mechanisms are also shown for seven large earthquakes of 21st century. White lines indicate the location of seismic profiles used in this study (15 profiles in the Andaman Sea; one profile (CGGV010) off of central Sumatra). The yellow rectangle marks the area of focus of this study, shown in Figure 2. GSF: Great Sumatra Fault.

[4] The 2004 Great Sumatra-Andaman earthquake ($Mw = 9.3$) ruptured >1300 km of the fore-arc region from Simeulue Island all the way to northern tip of Andaman Island [*Subarya et al.*, 2006], inducing stress on the GSF [*McCloskey et al.*, 2005; *Cattin et al.*, 2009, *Sevilgen et al.*, 2012] and making the northward extension of the GSF, a region of high seismic risk [*Cattin et al.*, 2009]. Therefore, understanding the nature of this sliver strike-slip fault is fundamental to the geodynamics of the region, as well as seismic hazard. In order to improve our understanding of the dynamics of the Andaman Sea region, we present 16 high-quality deep seismic reflection profiles starting from north of Banda Aceh near 6°N up to 11.5°N, which, along with bathymetry, gravity, and seismicity data, provide insight about the nature of these different faults and their interaction.

2. Tectonic Setting

[5] In order to understand the relationship between different faults in the region, it is important to discuss its tectonic history and major structural features. We first discuss the early formation of the Sumatra-Andaman subduction zone, then continue with a brief discussion on volcanism, address the obliquity of convergence, and identify the major structural features that we consider in this paper.

2.1. Tectonic History/Formation

[6] Subsequent to its splitting from eastern Gondwanaland, India separated from Australia in the Cretaceous time and took a spectacular flight northward, enhancing the convergence rate and broadening the subduction along the Eurasian margin, which seems to have already existed during the Permian time [*Katili*, 1973] (Figure 3). During this time, the subduction zone was dipping toward the NE and might have existed within or west of Sumatra, whereas in the Triassic-Jurassic period, the subduction zone moved toward the Indian Ocean. By the Tertiary time, the subduction margin reached a length of 6000 km [*Katili*, 1975].

[7] Around 59 Ma ago, the northern corner of greater India hit Eurasia during the initial collision causing the Indian plate to rotate anticlockwise until 55 Ma [*Klootwijk et al.*, 1992] (Figure 3). Between 55 and 45 Ma, India was indenting the Eurasian margin and rotating the subduction in a clockwise direction, increasing the obliquity of the subduction. At 44 Ma, India collided with Eurasia, leading to the
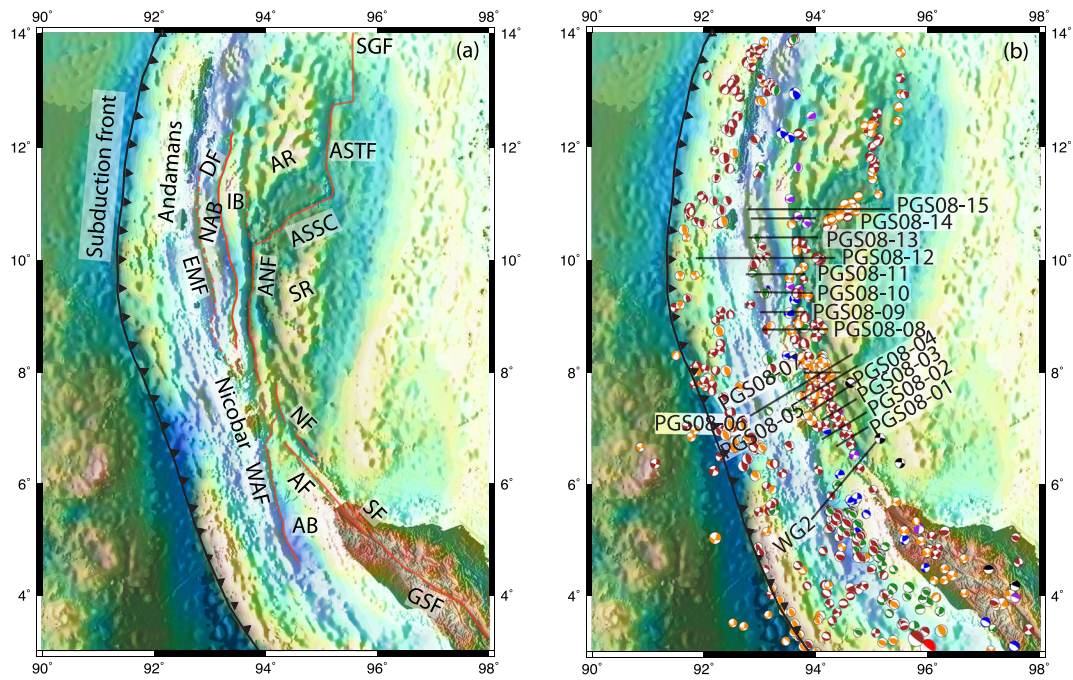
Figure 2. Combined bathymetry and gravity image of the Andaman Sea region showing (a) different tectonic features. AB: Aceh fore-arc basin, WAF: West Andaman Fault, AF: Aceh Fault, GSF: Great Sumatra Fault, SF: Seulimeum Fault, NF: Nicobar Fault, ANF: Andaman-Nicobar Fault, ASSC: Andaman Sea Spreading Centre, ASTF: Andaman Sea Transform Fault, SGF: Sagaing Fault, AR: Alcock Rise, SR: Sewell Rise, EMF: Eastern Margin Fault, DF: Diligent Fault, IB: Invisible Bank, NAB: Nicobar Andaman Forearc Basin. (b) Recent earthquakes with their fault plate solutions for different depths: Orange: 0–20 km; Red: 21–40 km, Green: 41–60 km; Blue: 61–80 km; Purple: 81–100 km; Black: 101–120 km. The black lines indicate the positions of seismic profiles used in this study.

development of the strike-slip sliver fault as the Sagaing Fault and West Andaman Fault in the east [*Peltzer and Tapponnier*, 1988]. The volcanic arc may have been east of these faults along the Mergui Ridge and on mainland Sumatra. The increasing oblique convergence might have moved the volcanic arc farther west and led to the extension in the Mergui Basin in late Oligocene between the volcanic arc and the Malaya Peninsula.
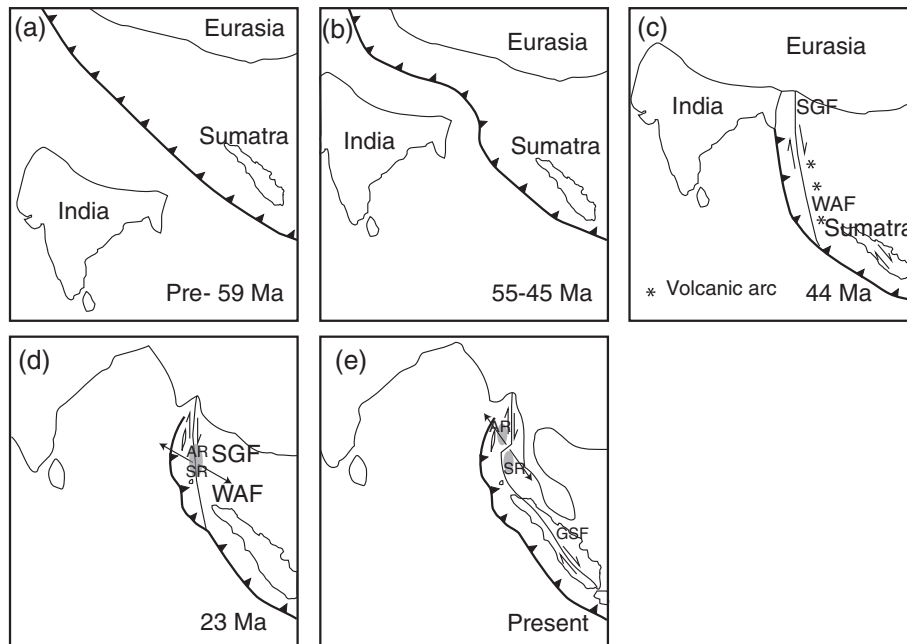

Figure 3. Map diagram illustrating the tectonic history of the Sumatra subduction and the Andaman Sea.

[8] By early Miocene, ~23 Ma, the plate convergence was oblique enough that the rifting moved westward close to the sliver fault and volcanic arc, leading to coincident seafloor spreading (~ 7 mm/yr) and volcanism forming the Alcock and Sewell Rises [*Curray*, 2005]. With continuing rotation of the arc, the direction of extension changed from 310° to 335° between 32 and 15 Ma and stabilized at 335° azimuth [*Curray*, 2005]. Around 15–16 Ma, the rifting jumped east of the volcanic arc and the Eastern Basin with E-W extension between the Alcock/Sewell Rises and the Malaya Continental Peninsula. About 4.5 Ma, spreading in the Central Andaman Sea initiated separating the Alcock and Sewell Rises [*Kamesh Raju et al.*, 2004]. The Great Sumatra Fault seems to have been active for the last 2 Ma [*Sieh and Natawidjaja*, 2000].

2.2. Volcanism/Volcanic Arc

[9] Although we have very little information about the volcanic arc in the Andaman Sea, volcanic rocks on mainland Sumatra provide some information about the history of volcanism in this region. Geochemical data suggest that volcanism in Sumatra initiated during the pre-Tertiary period [*Rock et al.*, 1982], but its intensity went up rapidly during the Tertiary period. In the Paleocene period, a volcanic arc was active along the southern margin of the Sunda microplate [*Crow*, 2005], and at the same time another inner arc was situated where the North Sumatra back-arc basin lies. *Crow* [2005] has suggested that in the late mid-Eocene period, volcanic rocks were distributed along the west coast of Sumatra and volcanic rocks in the Aceh area might have resulted from back-arc volcanism [*Cameron et al.*, 1980]. Late Miocene-Pliocene volcanism was particularly active in southern Sumatra [*Crow*, 2005].

[10] Quaternary volcanoes are irregularly distributed along and across the arc and mostly found north of the volcanic arc [*Rock et al.*, 1982]. A series of volcanoes are present along the western boundary of Sumatra. The locus of the hinge points of these volcanoes demonstrates a curvilinear shape, which surprisingly switches back and forth pivoting the trend of the main GSF [*Sieh and Natawidjaja*, 2000]. The proximity of the chain of volcanoes and the GSF indicates that there might be a correlation in the origin of these structural elements. At the northern tip of Sumatra, the volcanic arc aligns with the Seulimeum fault as it enters the sea. *Ghosal et al.* [2012] suggest that this arc shifts farther northward in a pull-apart basin whereas the main active strand of the GSF follows the Aceh Fault strand.

2.3. Obliquity/Rates of Convergence

[11] From 59 Ma to 44 Ma, India was indenting the Asian margin and causing the clockwise rotation of the subduction zone thus increasing the obliquity of convergence [*Curray*, 2005]. The arcuate western margin of the Sunda microplate imposes obliquity upon the direction of the subducting Indo-Australian plate. The direction of subduction varies from 90° near Java to 60° in central Sumatra, reduces to 45° in northern Sumatra, and becomes almost parallel to the Andaman Islands farther north. The convexity of the western margin of the Sunda microplate not only influences the direction of convergence of the subducting oceanic plate, but it immensely affects the rate of subduction as well. The rate of convergence is 63 mm/yr near the Java trench,

and 50 mm/yr near the Nias Island, becomes 45 mm/yr at the NW of Sumatra, and reaches 39 mm/yr near the Andaman Island [*Chlieh et al.*, 2007, *Cattin et al.*, 2009] (Figures 1, 2). Sparse geodetic data indicate variations in the rate of convergence from 14 mm/yr to 34 mm/yr north of 8°N [*Gahalaut et al.*, 2006; *Paul et al.*, 2001].

2.4. The Sliver Fault

[12] With increasing obliquity, the initial sliver fault formed, probably in the middle to late Eocene, around 44 Ma [*Curray et al.*, 1979; *Curray*, 2005]. The sliver fault was identified as the Sagaing Fault in Myanmar, connected to the WAF and GSF systems to the south [*Curray*, 2005] through transform faults and the spreading center in the central Andaman Sea basin (Figure 2a). *Curray* [2005] suggested that the WAF may have been primarily a reverse fault, forming the Invisible Bank, and uplifting older fore-arc basin sediments north of the spreading center, but is a strike-slip south of the spreading center all the way to northern Sumatra. The WAF was also interpreted to represent an earlier sliver fault off northwest Sumatra running into the Mentawai Fault [*Diament et al.*, 1992], while the Sumatra fault system is the presently active sliver fault.

2.5. The Andaman Sea Spreading Center

[13] The Andaman Sea is a complex back-arc extensional basin formed by transtension soon after the collision of India with Eurasia in Paleogene time [*Peltzer and Tapponnier*, 1988]. The Central Andaman Sea basin is ~118 km wide and formed in the last ~4.5 Ma [*Kamesh Raju et al.*, 2004]. Adjacent to the Andaman Sea, the convergence direction between the India and Eurasian plates is approximately parallel to the arc, and without the component of opening of the Andaman Sea, there would be no subduction, only lateral motion [*Curray*, 2005]. Major stratigraphic changes occurred on the Andaman-Nicobar ridge and in the Mergui basin at about 4–5 Ma, the time when rifting began separating the Alock and Sewell Rises and the time the slivers strike-slip fault moved onto land [*Sieh and Natawidjaja*, 2000].

3. Seismicity

[14] The Andaman-Sumatra subduction region is one of the most seismically active regions on the Earth [*Engdahl et al.*, 2007]. In the last 7 years, there have been five $Mw > 8.2$ earthquakes in this region (Figure 1) [*Briggs et al.*, 2006]. The recent activity started in 2004 with the 21st century's largest magnitude earthquake, $Mw = 9.3$, on 26 December, which produced a devastating tsunami across the Indian Ocean. The second earthquake, $Mw = 8.7$, followed 3 months later, on 28 March 2005 near Nias Island 150 km south. After 3 years, a $Mw = 8.5$ earthquake struck on 12 September 2007 at 800 km farther south near Bengkulu [*Konca et al.*, 2008]. A twin strike-slip earthquake of $Mw = 8.6$ and $Mw = 8.2$ occurred on 11 April 2012 just south of the 2004 earthquake on the subducting Indo-Australian plate [*Duputel et al.*, 2012].

[15] The 2004 and 2005 events totaled a rupture length of 1700 km and coseismic displacements of up to 25 m [*Chlieh et al.*, 2007; *Rhie et al.*, 2007; *Fujii and Satake*, 2007]. As a result, these earthquakes have caused large stress perturbations in the region. *Cattin et al.* [2009] have calculated the static Coulomb stress change distribution along

the Sumatra-Andaman-Sagaing fault system after the 2004 and 2005 earthquakes and suggested that these events inhibit failure north of the ASSC and on the Sagaing Fault, while failure is encouraged along the ASSC, the WAF, and the GSF systems. These results are consistent with the temporal evolution of earthquake distribution and focal mechanisms, before and after the main events, and explain observed swarms in the Andaman Sea [*Lay et al.*, 2005]. The maximum stress change lies at the northern portion of the Great Sumatra Fault (GSF) [*Cattin et al.*, 2009; *McCloskey et al.*, 2005], which has been rather silent in the recent past, and may rupture in the near future producing large earthquakes both on land and offshore. It is therefore important to study the GSF and its offshore extension farther north.

[16] Figure 1 shows seismicity since 1977 [*Pesicek et al.*, 2010]. Aftershocks of the 2004 earthquake dominate the seismicity from the north of Sumatra to the Andaman Islands. A cluster of aftershocks occurred at the intersection of WAF and the seaward extension of GSF [*Lay et al.*, 2005; *Kundu et al.*, 2012]. Earthquakes also define the Andaman Sea Spreading Centre (ASSC) and how it links the WAF-GSF with the Sagaing Fault in Myanmar through the Andaman Sea Transform Fault (ASTF). It is noticeable that the earthquakes occur across the whole fore-arc region. The earthquakes occur in the shallower part of the fore-arc region, up to the trench, north of the 2004 event and south of the 2007 event, while most of the events occur deeper beneath the fore-arc highs and basins between those two earthquakes. Although seismicity defines the GSF on land, it remains relatively weak as compared to the seismicity associated with subduction thrusting. Focal mechanisms suggest that the subduction earthquakes are generally thrust events. The earthquakes associated with the GSF, its northward extension, the transform fault in the Andaman Sea, and the Sagaing fault are mainly strike-slip earthquakes with some normal earthquakes; those along the spreading center are normal events (Figure 2b). The earthquakes on the oceanic plate, as the 11 April 2012 event, occur along reactivated N-S fracture zones and are left-lateral strike events [*Abercrombie et al.*, 2003; *Deplus et al.*, 1998; *Deplus*, 2001; *Delescluse et al.*, 2012]. The strike-slip events beneath the fore-arc also lie along reactivated and subducted fracture zones. We shall discuss these and other focal mechanisms in the light of seismic reflection images.

4. Seismic Data

[17] We have access to 16 deep seismic profiles crossing the northward extension of the GSF starting from north of Banda Aceh up to the Andaman Islands (Figures 1 and 2). Profile WG2 was acquired by WesternGeco in 2006 on board the seismic vessel Geco Searcher, as a part of a deep seismic study of the 2004 great Sumatra-Andaman earthquake rupture zone [*Singh et al.*, 2008; 2012; *Chauhan et al.*, 2009]. It was acquired using two streamers: one 12 km long towed at 15 m to image deep structures, and the other 5.5-km long towed at 7.5 m to provide high-resolution seismic images of the near surface sediments and faults. An array of 48 air guns with a total volume of 166.67 L was towed at 15 m to provide the energy source for deep seismic imaging. The shot interval was 50 m and the record length was 20 s. The profile traverses the whole Sumatra subduction system, starting from the

oceanic plate in the Indian Ocean, crossing the deformation front, accretionary wedge, fore-arc high, fore-arc basin, the Sumatra continental platform, the GSF, and the volcanic arc up to the Mergui Basin in the Andaman Sea. The data were processed using both conventional [*Singh et al.*, 2012] and advanced processing techniques [*Ghosal et al.*, 2012] to obtain migrated time and depth images, respectively.

[18] The other 15 profiles (Figure 2) were acquired by Petroleum Geo-Services (PGS) as part of a speculative survey for oil and gas exploration in 2008. An 8 km long streamer was towed at 7.5 m water depth and an array of air guns with a total volume of 81.93 L was towed at 6 m to provide the energy source. The shot interval was 25 m and the record length was 9 s. The data were processed using conventional processing techniques up to prestack time migration. Two of the profiles (PGS08-06, PGS08-12) traverse the whole subduction system; the rest traverse the northward extension of GSF at different locations. The northernmost profiles, PGS08-14 and PGS08-15 also cross the Andaman Sea spreading center, linking the deformation process due to subduction with the back-arc spreading in the Andaman Sea.

[19] We have also used one of the deep seismic profiles (CGGV010) acquired by CGGVeritas in 2009 from the Mentawai fore-arc basin region [*Mukti et al.*, 2012] (Figure 1) to compare with the images from the Andaman fore-arc basin. The profiles were acquired using three streamers, one 15 km long towed at 22.5 m water depth and two 6 km long towed at 7.5 m and 15 m depths. An array of air guns with a total volume of 157.32 L was towed at 15 m depth to provide low frequency energy for deep penetration. The data from the three streamers were combined to obtain deep seismic images. The data were resampled to 4 ms and migrated using the Kirchhoff prestack time migration technique [*Singh et al.*, 2011a, 2011b].

[20] The main focus of this paper is to study the northward extension of the GSF, and therefore, we only use parts of the seismic profiles that contain features that interact with the GSF, namely the WAF, the volcanic arc, and the Andaman Sea spreading center (ASSC). Although seismic images along profile WG2 and CGGV010 are up to 20 s, we only show images down to 9 s to be consistent with the PGS data. The latitude and longitude of each profile are given in Table 1. We also plot gravity and bathymetry data along each profile to discuss the possible origin of the different features. The gravity data are taken from satellite altimetry [*Sandwell and Smith*, 2009], and we have used the seafloor reflection arrival time and a water velocity of 1.5 km/s to determine the bathymetry along the profiles. In order to relate seismic images with active deformation, we also show the projection of hypocenters along the profiles. In the next section, we first discuss five long profiles to give the general picture of structures in the region and show how they are linked, then focus on the details of the main features, such as the WAF and the GSF.

5. Seismic Results

5.1. Profile WG2

[21] Results from the WG2 profile have already been published elsewhere [*Chauhan et al.*, 2009; *Singh et al.*, 2012; *Ghosal et al.*, 2012], but we briefly discuss different elements observed along it. We use this profile as a reference profile, because the different features of interest are well separated along it. Furthermore, crustal structure using seismic

Table 1. Start and End Coordinates of All Seismic Profiles Used in This Study

	Start		End	
Profile	Latitude	Longitude	Latitude	Longitude
CGGV010	2.13°S	99.25°E	1.50°S	100.00°E
WG2	5.40°N	93.85°E	6.66°N	95.25°E
PGS08-01	6.61°N	94.39°E	7.00°N	94.99°E
PGS08-02	6.83°N	94.11°E	7.28°N	94.88°E
PGS08-03	7.22°N	94.11°E	7.57°N	94.78°E
PGS08-04	7.28°N	94.11°E	7.89°N	94.78°E
PGS08-05	7.56°N	93.72°E	8.11°N	94.78°E
PGS08-06	7.25°N	92.90°E	8.38°N	94.75°E
PGS08-06	8.00°N	93.83°E	8.00°N	94.39°E
PGS08-08	8.80°N	93.06°E	8.80°N	94.22°E
PGS08-09	9.10°N	93.06°E	9.10°N	93.83°E
PGS08-10	9.40°N	92.94°E	9.40°N	93.89°E
PGS08-11	9.70°N	92.67°E	9.70°N	93.83°E
PGS08-12	10.00°N	91.85°E	10.00°N	94.38°E
PGS08-13	10.45°N	92.83°E	10.45°N	94.10°E
PGS08-14	10.75°N	92.88°E	10.75°N	94.00°E
PGS08-15	10.98°N	92.75°E	10.98°N	95.43°E

tomography and gravity data is well constrained along this profile [*Singh et al.*, 2012], which helps to interpret the gravity data and seismic reflection data along other profiles in terms of crustal structure and allows us to distinguish between sedimentary structures, continental crust, and igneous (volcanic and oceanic) crust. At the southwest end of the profile (Figure 4), we observe a 30 km wide fore-arc high that rises up to 300 m water depth. There are up to 1.5 s two-way travel time (TWTT) thick recently deformed sediments at its shallowest part, suggesting that the fore-arc high has been folded and uplifted. These deformed sediments are underlain by poorly reflective accretionary wedge sediments that contain

some seaward-verging parallel dipping reflections, suggesting that they were formed by stacking of accretionary prism sediments. Their accretionary wedge sedimentary origin is further confirmed by low *P* wave velocity determined using ocean bottom seismometer tomographic studies [*Chauhan et al.*, 2009], low gravity anomaly, and shallow bathymetry between 0 and 70 km distance range (Figure 4). These accretionary wedge sediments are underlain by a set of landward verging reflectors that emerge at the northeast toe of the fore-arc high, at the southwest margin of the Aceh fore-arc basin. Using combined seismic reflection and refraction data, *Chauhan et al.* [2009] suggested that these reflectors are the back thrust and lie at the continental back stop, and are the subsurface manifestation of the West Andaman Fault (WAF). *Singh et al.* [2011a] have imaged similar back thrusts farther south in the Mentawai region, the Mentawai Fault Zone (MFZ). *Mukti et al.* [2012] suggest that the MFZ is about 15 Ma old and acts as a contractional boundary for the deformation of the Sumatra fore arc.

[22] The Aceh fore-arc basin is 20 km wide and lies at 2200 m water depth. It contains about 1 s of thick horizontal sediment and is underlain by a strong reflective basement. The high *P* wave velocity of the basement suggests that the Aceh basin is floored by the Sumatra continental crust [*Chauhan et al.*, 2009; *Singh et al.*, 2012]. The Sumatra platform is ~60 km wide and lies at 1500 m water depth. The high *P* wave velocity there suggests that it is also of continental origin and hence an offshore extension of the mainland continental Sumatra. Note the correlation between the gravity and bathymetry data for the continental crust, between 100 km and 160 km (Figure 4). There is a small basin at its southern end, which *Berglar et al.* [2010] have suggested to be formed by a now inactive strike-slip fault.
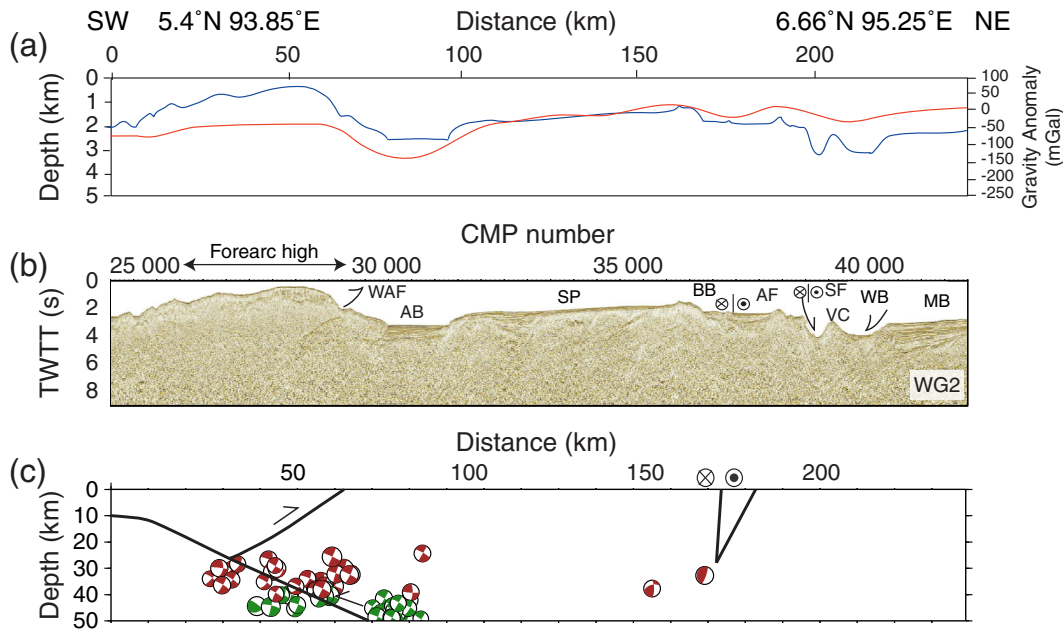

Figure 4. Profile WG2: (a) Gravity anomaly (red) and bathymetry (blue), (b) seismic reflection image, and (c) hypocenters of earthquakes projected along profile WG2 in a 50 km wide zone along with their rotated fault plane solutions. The black lines indicate the approximate positions of the plate interface and back thrust. West Andaman Fault (WAF) is a back thrust. AB: Aceh Basin, SP: Sumatra Platform, AF: Aceh Fault, SF: Seulimeum Fault, VC: Volcanic Centre, BB: Breueh Basin, WB: Weh Basin, MB: Mergui Basin.
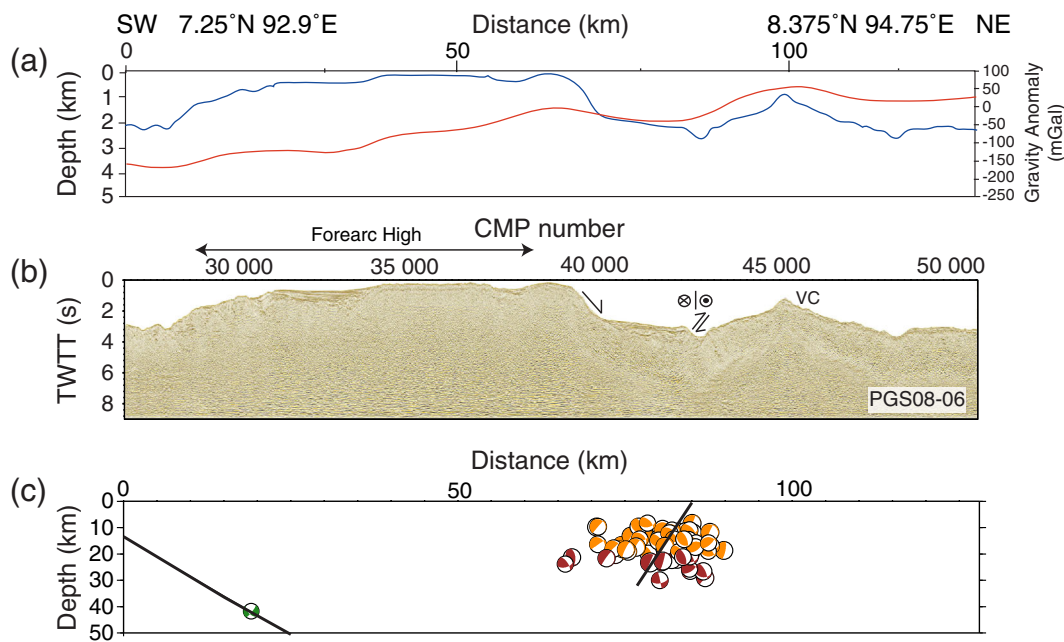
Figure 5. Profile PGS08-06: (a) Gravity anomaly (red) and bathymetry (blue), (b) seismic reflection image, and (c) hypocenters of earthquakes projected along profile in a 20 km wide zone along with their rotated fault plane solutions. The black lines indicate the approximate positions of the plate interface and back thrust. VC = Volcanic Cone.

[23] Northeast of the Sumatra continental platform, there are two ~20 km wide basins. The southern Breueh basin lies at 2000 m water depth. The recent sediments in Breueh Basin are V-shaped and their thickness varies from 0.5 s to 1.5 s. The SW bank of the basin is bounded by a normal fault and a rotated fault block. There is a push-up ridge in the thickest part of the basin, suggesting a complex deformation pattern. The bathymetry data shows that this push-up extends farther northeastward [*Ghosal et al.*, 2012]. The basement beneath the push-up ridge is faulted like a knife-edge and has a vertical offset of about 200 ms, which led *Ghosal et al.* [2012] to suggest that it is the site of the main branch of the strike-slip Aceh fault, the southern strand of GSF on land. The high *P* wave velocity beneath the basin suggests the presence of continental crustal material.

[24] The SW margin of the northern Weh basin is bounded by two tilted fault blocks without any recent sediments; the steep (~75°) scarp with more than 800 m relief suggests the presence of active normal faulting. A 500 m high volcano is present at the center of the basin. Bathymetry data show that there are at least two more volcanoes farther northwest in the basin [*Ghosal et al.*, 2012] aligned in the NE direction. Toward mainland Sumatra, volcanoes are aligned in the NE direction, but they lie farther southeast in alignment with the fault blocks. Since there is no evidence of volcanic material NE of the scarp, the volcanic center seems to have shifted farther northeast to the center of the Weh Basin. A veneer of ~300 ms thick sediments is present southwest of the volcano, where the apex of deposition has shifted northeastward and is likely to be of volcano-clastic origin. No coherent reflections are observed beneath the volcano. The coherent reflections from sediments in the Weh basin are very thin (up to 500 ms), suggesting that this deep basin is recent. In the northeast, the basin is bounded by a basinward dipping normal fault

with a slope of 45°, suggesting that this fault should be the antithesis fault of the main fault southwest of the basin. A thick (2.5 s) sedimentary basin tilting toward the Weh basin is present in the Mergui basin, which seems to have undergone some deformation. A positive gravity anomaly in this region suggests the presence of a thinned continental crust, which is supported by deep seismic reflection and refraction results [*Singh et al.*, 2012].

[25] On land, the Seulimeum fault, the northern strand of the GSF, follows the volcanic arc toward the NW. Based on the rhombic shape of the 60 km long Weh basin, *Ghosal et al.* [2012] suggested that the basin was formed by a releasing step over along the Seulimeum fault. They argued that southern strand, the Aceh fault, is straight for ~200 km offshore and is active, and hence, it could be the site of a large earthquake. On the other hand, the Seulimeum fault is segmented and thus likely to produce smaller earthquakes. The projection of hypocenters along the profile defines position of the plate interface beneath the fore arc and the active Aceh Fault.

5.2. Profile PGS08-06

[26] This profile traverses the Sumatra subduction system more or less orthogonally north of the Great Nicobar Island and passes through the aftershock clusters observed after the 2004 earthquake (Figure 5). A piggyback basin is observed on the SW side of the profile. The fore-arc high is nearly flat and rises up to 200 m water depth. There is a small basin toward the NE. The tilted sediments indicate that it might be a piggyback basin formed by tilting/uplifting of the block in the northeast. The reflection characteristic of the seafloor and the lack of reflectivity underneath suggest that it might be capped by carbonates. The fore-arc high is about 60 km wide, much wider than that along profile WG2. There is a 1200 m deep scarp on its NE side. Poorly imaged northeastward-tilted
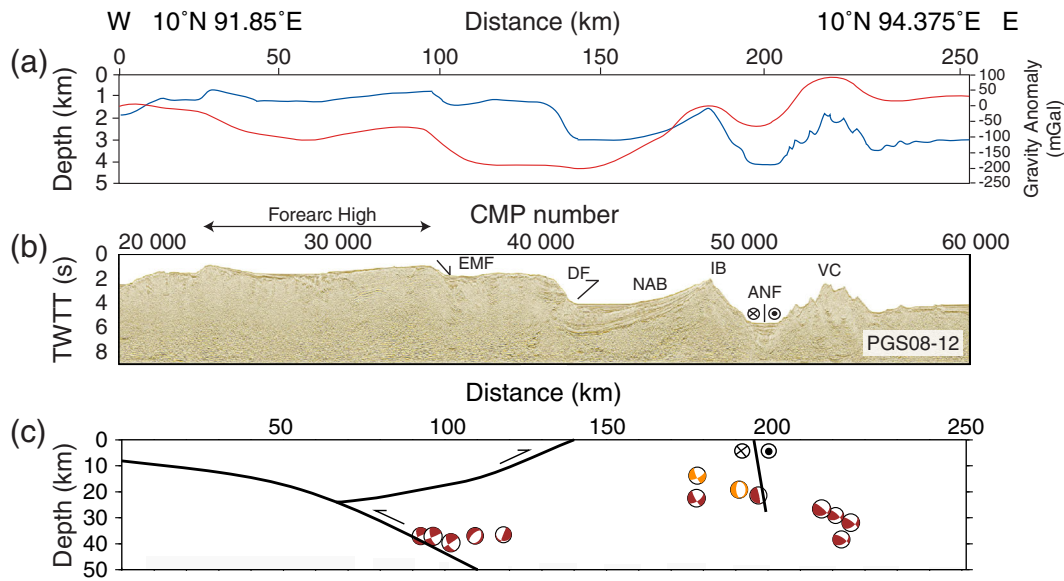
Figure 6. Profile PGS08-12: (a) Gravity anomaly (red) and bathymetry (blue), (b) seismic reflection image, and (c) hypocenters of earthquakes projected along profile in a 50 km wide zone along with their rotated fault plane solutions. The black lines indicate the approximate positions of the plate interface and back thrust. EMF: Eastern Margin Fault, DF: Diligent Fault, IB: Invisible Bank, NAB: Nicobar Andaman Forearc Basin, ANF: Andaman-Nicobar Fault (previously interpreted as WAF), VC: Volcanic Complex.

sediments beneath the scarp suggest normal faulting. At the base of the scarp, a 7 km wide northeastward-tilted basin is present. The sediments are up to 600 ms thick and are deformed in a pattern similar to the deformation observed in the Breueh basin along profile WG2. There is a small push-up ridge at the northeast of this basin with sediments tilting southwestward. The ridge is underlain by a northeastward verging thrust bounding a tiny basin, which itself is bounded by a southwest dipping normal fault at its northeast side. It is difficult to interpret the precise locations of the back thrust and the strike-slip fault, but this narrow valley might be the site of the Nicobar fault, which means both back thrust and strike-slip faults are close to each other. The low gravity anomaly and shallow bathymetry suggest that the western part of the fore-arc high is underlain by a thick sedimentary sequence. A linear increase in gravity northeastward along the fore-arc high is indicative of the increasing presence of continental or igneous material underneath, as suggested by the combined bathymetry and gravity data along profile WG2.

[27] There is a broad 20 km wide conic feature farther NE that rises up to 800 m water depth. Up to 100 ms thick sediments are present along the flank of this cone, which is otherwise devoid of sediments. It is therefore difficult to say if this cone is of continental or volcanic origin. Although it coincides with a gravity anomaly of +50 mgal, its high bathymetry suggests the presence of some continental material underneath, at least on its western side. Farther northeast of the cone, there is a small valley bounded by a thin sediment capped ridge farther northeast. Relatively high gravity and low bathymetry at the northeast end of the profile are suggestive of igneous crust.

[28] Even though we do not observe a clear strike-slip fault along this profile, a cluster of earthquakes occurred in 2004–2005 in this broad zone (Figure 5c). Although most of the earthquakes have strike-slip motion, some of them have normal as well as thrust components, indicative of a

complex deformation, possibly due to the interaction of the compressive WAF and strike-slip GSF leading to enhanced seismicity. The hypocenters of these earthquakes lie between 10 and 35 km depth. We have no estimation of the crustal thickness along this profile, but it should be less than, or the same as, that along profile WG2 (20–25 km) [*Singh et al.*, 2012], meaning that some of the earthquakes occur in the mantle, and hence the deformation is on the lithospheric scale as subduction related earthquakes would be much deeper (60–80 km depth) here. Lithospheric-scale faulting near a volcanic arc is surprising, supporting the idea that there might not be any genetic link between volcanic arc process and sliver plate deformation as suggested by *Sieh and Natawidjaja* [2000]. The volcanic melt seems to have been produced by melting at depth (60–80 km) [*Singh et al.*, 2012] and passed through the mantle and crust without affecting the rheology, and therefore, the volcanoes must be very superficial features along the volcanic arc. On the other hand, *Kundu et al.* [2012] and *Kamesh Raju et al.* [2012] suggest that the volcanism and strike-slip faults are linked, and the 2005 swarm was due to stress induced by the 2004 earthquake.

5.3. Profile PGS08-12

[29] This profile is an E-W profile at 10°N, between Little Andaman and Car Nicobar Islands. The fore-arc high has a saddle with thin sediments dipping eastward, possibly formed by an out-of-sequence eastward dipping thrust in the west (Figure 6). There are some deformed sediments on the eastern side of the saddled basin, possibly indicating the passage of a strike-slip fault in the region. Farther east, the fore-arc high dips gently westward. The absence of reflection between CMPs 25,000 and 35,000 and the subhorizontal topography suggest that it is a carbonate platform and has now subsided to ~1000 m water depth, or highly deformed sediment. The fore-arc high is 140 km wide, the widest along
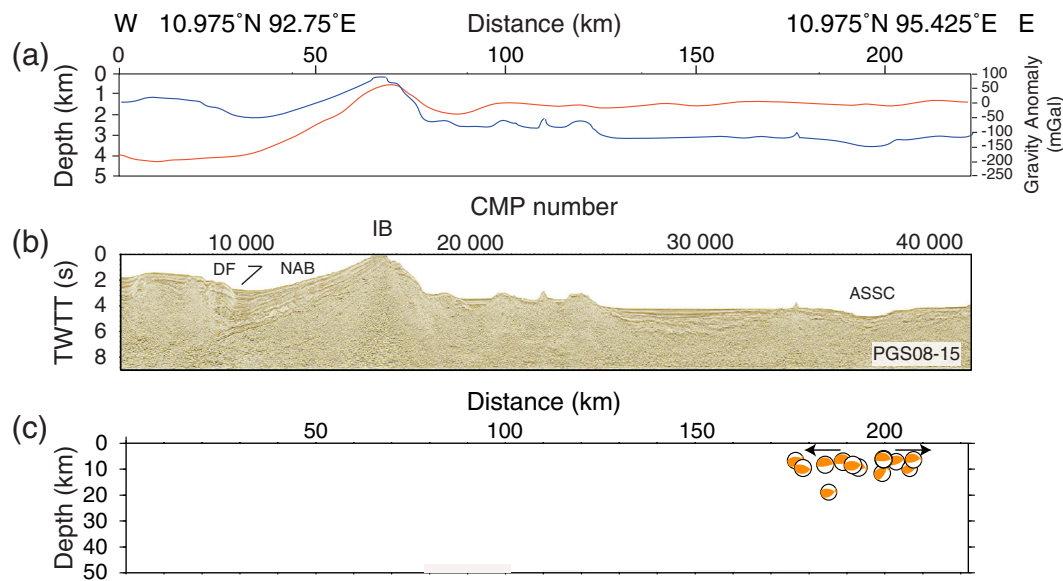
Figure 7. Profile PGS08-15: (a) Gravity anomaly (red) and bathymetry (blue), (b) seismic reflection image, and (c) hypocenters of earthquakes projected along profile in a 20 km wide zone along with their rotated fault plane solutions. DF: Diligent Fault, IB: Invisible Bank, NAB: Nicobar Andaman Forearc Basin, ASSC: Andaman Sea Spreading Center.

the Andaman-Sumatra margin. Although the bathymetry remains similar along the fore-arc high, the gravity decreases eastward, particularly between 100 and 135 km distance range (Figure 5), suggestive of increasing sediment thickness eastward. The Eastern Margin Fault (EMF) has produced a small basin at its footwall that lies at ~1350 m water depth and contains deformed sediments. The presence of eastward dipping sediments east of the EMF suggests that the fore-arc high was uplifted by a thrust fault farther east. Although the water depth remains the same, more than 2 s thick eastward dipping deformed sediments are imaged between CMP 39,000 and 41,500. There is an 800 m steep scarp at CMP 41,800, which previously has been interpreted as Diligent Fault (DF) [*Curray*, 2005; *Cochran*, 2010]. The low gravity anomaly suggests the presence of thick sediments west of the scarp. There is a ~20 km wide basin at the foot of this scarp, where the upper 300 ms thick sediments are horizontal, underlain by thick (1.5 s) westward dipping sediments that pinch out toward the top of a rise at 1800 m water depth, which corresponds to the Invisible Bank (IB). It is possible that the thick sediments observed between CMP 39,000–41,500 belong to this lower sequence that has been uplifted by a thrust fault near the scarp. Indeed, underneath these sediments, there seems to be a set of thrust faults (marked by sharp amplitude blanking) that arrives at the western margin of the basin. Uplifted sediments on the fore-arc high and back thrusts separating the Aceh fore-arc basin were also observed on profile WG2 (Figure 4). If the structures on profile PGS08-12 are similar to those on profile WG2, two inferences can be drawn: (1) The Diligent Fault, a back thrust, is similar to WAF; and (2) the fore-arc basin is underlain by a continental crust. The eastward increase of the gravity anomaly toward the Invisible Bank (IB) agrees with this last inference. If this is the case, then the IB should represent the continental margin of the Malaya Peninsula. Some rock samples collected from the IB do suggest a continental origin [*Roy and Chopra*, 1987].

A steep scarp on the east side of the IB and tilted on-lapping sediments in the west of the IB suggest that it is a large continental fault block, with a rift basin lying to the east of the rise. There are some reflections below what looks like the base of the sedimentary sequence on the slanting rise. The earthquake hypocenters beneath the DF show steeply dipping thrust mechanism and two complex strike-slip mechanisms. Their depth is ~40 km, and hence, it is difficult to say whether they are due to thrusts on subducting plate or back thrusts.

[30] A knife-edged vertical fault, having a vertical offset of about 100 m, is visible in the center of a 2 s thick basin at 4000 m water depth east of the rise, which we suggest is due to a strike-slip fault. The presence of a strike-slip fault in a deep basin indicates transtensional deformation along the fault, similar to the Seulimeum fault on profile WG2. Farther east, a large cone-shaped feature with several volcano-like structures is observed, and seems to be of volcanic origin as there is no sediment on them. The high gravity anomaly further confirms their volcanic origin, suggesting that the volcanic arc lies on the east of the strike-slip fault. Farther east, there is a small basin, indicating the possible presence of an old strike-slip fault. The sediment thickness increases farther eastward. The absence of Moho reflection underneath suggests that the crust is either thick or that the Moho is a transition in this region. However, deep water and zero free gravity anomaly suggest that the crust is likely to be of igneous origin. Hypocenters beneath the strike-slip fault show strike-slip earthquakes at 10–20 km depth. Surprisingly, there are four earthquakes at 40 km east of the volcanic cone with normal fault plane solutions. It is possible that their locations are offset by 50 km toward the east or that their depths are offset by 20–30 km, but if their locations and depths are correct, they might be associated with rifting at the spreading center 30–40 km farther north as their strikes are the same as that of the spreading center. *Kamesh Raju et al.* [2004] proposed the presence of a propagating rift, consistent with
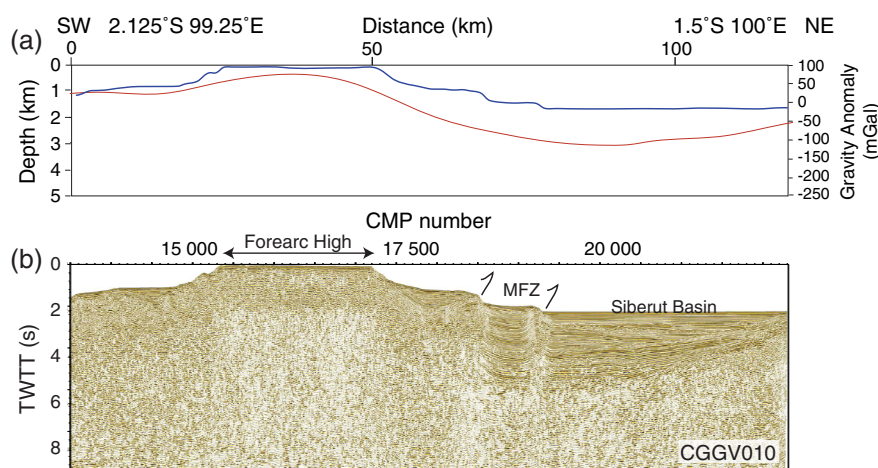
Figure 8. Profile CGGV10: (a) Gravity anomaly (red) and bathymetry (blue) and (b) seismic reflection image. MFZ: Mentawai Fault Zone. Location of profile off of central Sumatra, see Figure 1.

our interpretation. Deep normal faulting further suggests a lithospheric-scale deformation in the region, and hence the lithosphere must be cold and brittle.

5.4. Profile PGS08-15

[31] Profile PGS08-15 is the northernmost profile of this study and starts at the northeastern tip of Little Andaman Island. It therefore does not cross the fore-arc high but extends up to the Andaman Sea Spreading Center, providing a link between the fore-arc basin, strike-slip fault, volcanic arc, and spreading center. The Nicobar Andaman Forearc Basin at the western end of the profile contains 1.5 s thick sediments (Figure 7). There is a broad fold thrust imaged with a westward dipping blind thrust underneath, bounding the present day fore-arc basin, representing the Diligent Fault. A bottom-simulating reflector (BSR) is imaged along a part of the profile. Although the near-surface sediments in the fore-arc basin are nearly flat, the sediments underneath dip westward, similarly to those imaged along profile PGS08-12. The back thrust is weakly imaged at depth but one can trace it down to 7.5 s. The IB is flat and lies at 50 m. There are some bright reflectors (CMP 13,000–17,000) beneath the subparallel fore-arc basin sediments that might correspond to older sediments deposited on the continental margin of the Malaya Peninsula. The eastern slope is steep and drops to 3.2 s. There are some chaotic reflectors that pinch out along the slope. A push-up ridge with a flower structure at the east of the IB is suggestive of the presence of a strike-slip fault, but only a few strike-slip earthquakes occur in this area (Figure 2). There are three bathymetric features farther east, two of them have some sediment above them and hence are likely to be tilted fault blocks; the small central one looks like a volcanic cone. The young oceanic crust starts from CMP 27,000 and is covered by ~2 s thick sediments. The rift valley of the sedimented Andaman Sea Spreading Center (ASSC) could be observed between CMP 37,000 to 38,200 and contains inward dipping faults. The projection of the hypocenters along the profile suggests that the spreading center is seismically active.

5.5. Profile CGGV010

[32] Similar to the reference profile WG2, Profile CGGV010 is used to show the similarity between the fore-arc high, back

thrust, fore-arc basin, and the continental margin slope observed on the previously described profiles and with those studied in the Mentawai region [*Mukti et al.*, 2012], ~1000–1500 km farther southeast along the central and southern Sumatra margin. This profile crosses the subduction zone roughly orthogonally to the trench, just south of Siberut Island, along the locked segment of the Sumatra seismic gap [*Chlieh et al.*, 2007] (Figure 1). The fore-arc high is ~60 km wide, and its shallowest part is nearly flat and lies at 50 m water depth (Figure 8). In the southwest, it is bounded by a series landward dipping thrust faults whereas in the northeast, it is bounded by seaward dipping active back thrusts that define the Mentawai Fault Zone [*Mukti et al.*, 2012]. Two back thrusts are clearly imaged at the southwestern margin of the Siberut basin. *Mukti et al.* [2012] suggest that these back thrusts become progressively younger toward the northeast. On profile PGS08-15, we find similar progression of back thrusts toward the east (Figure 7).

[33] The Siberut fore-arc basin is ~60 km wide, and a significant part of it lies at 1700 m water depth. Sedimentary thickness in the fore-arc basin increases from 1 s TWTT in the northeast to 4 s TWTT in the southwest. A stratigraphic analysis of the basin sediments has been presented by *Mukti et al.* [2012]. The age of the recent sediments varies from Pliestocene to Oligocene-Early Miocene (~23 Ma). The oldest known sediments in the Siberut Basin are 40–45 Ma old, but some of sediments could be as old as 85 Ma [*Mukti et al.*, 2012]. The upper sediments are nearly flat whereas lower units dip southwestward and pinch out in the northeast, similarly to those imaged west of the Invisible Bank in the Andaman Sea. The crust beneath the fore-arc basin is of continental origin as a continental back-stop was imaged down to the intersection of the subducting oceanic plate [*Singh et al.*, 2011b]. The similarity between seismic images along profiles CGGV010, WG2, PGS08-12, and PGS08-15 (Figures 4, 6–8) suggests that the Invisible Bank and NAB represent a part of a fore-arc basin that was once attached to the Malaya peninsula, which has now rifted away due to the opening of the Andaman Sea around 23–32 Ma ago. It is possible that deeper sediments imaged beneath the NAB west of the Invisible Bank therefore could be as much as 85 Ma old. Since the distance between
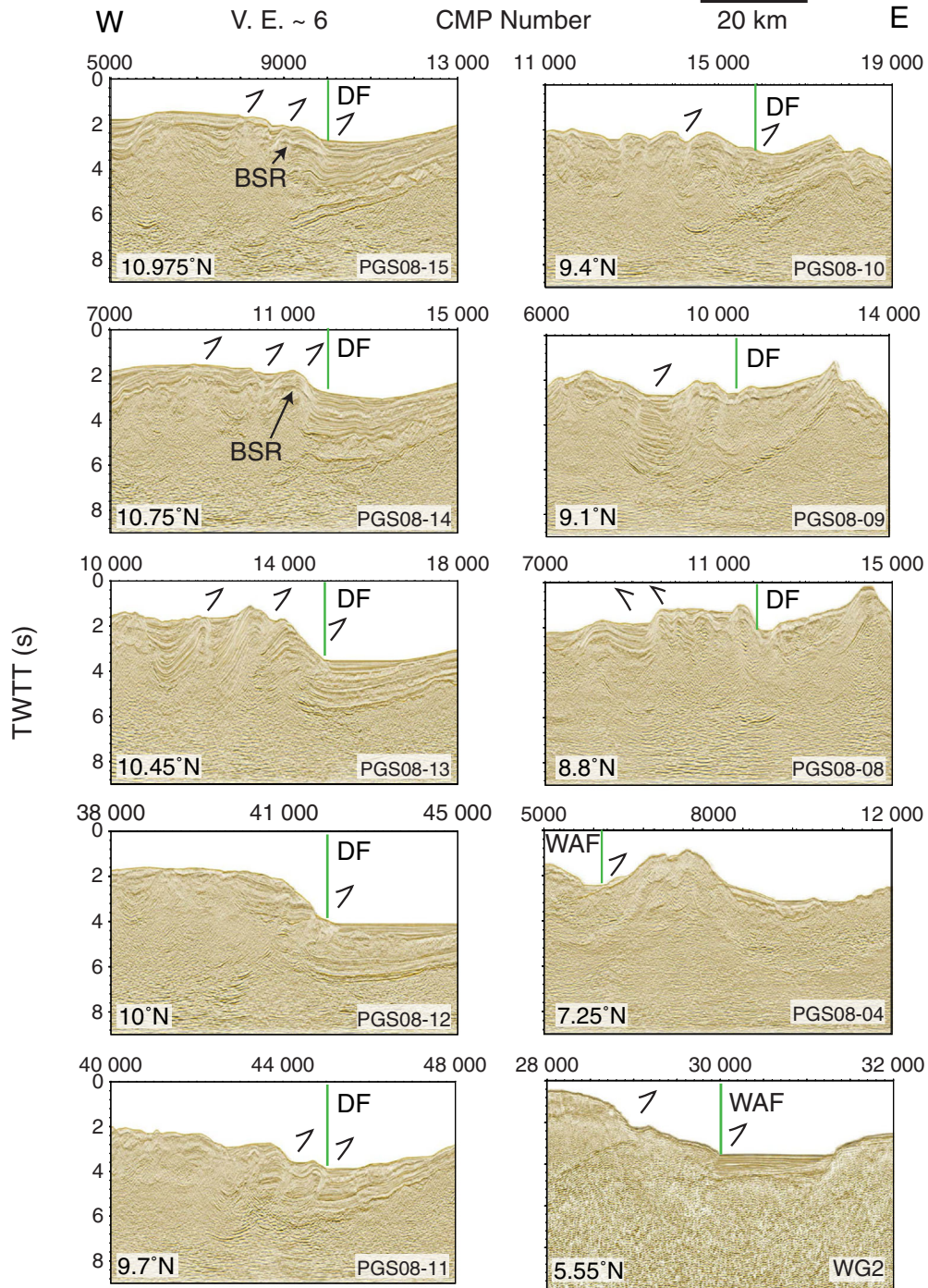
Figure 9. Seismic reflection images from north to south of the back thrust which has been interpreted as Diligent Fault (DF) in the north of Nicobar and West Andaman Fault (WAF) in the south. The green line indicates the surface arrival of the DF. BSR: Bottom-Simulating Reflector. All profiles are ~50 km long.

Andaman fore-arc basin and Siberut Basin is more than 1500 km, one has to be cautious with the above interpretation.

[34] The presented seismic profiles, combined with bathymetry and gravity data, highlight seven main features: (1) the fore-arc high, (2) back thrusts bounding fore-arc high and fore-arc basin (Figure 9), (3) the fore-arc basins underlain by continental crust, (4) the sliver strike-slip fault (Figure 10), (5) a rift system, (6) the volcanic arc, and (7) the ocean spreading center. First, we concentrate on

the details of the back thrust and strike-slip faults; then, we summarize our observations.

5.6. Back Thrust

[35] Figure 8 shows the seismic images of the observed back thrust from north to south along 10 profiles. In the north it has been interpreted as the Diligent Fault, whereas in the south as the West Andaman Fault. On the northernmost profile, PGS08-15, three back thrusts are observed. The
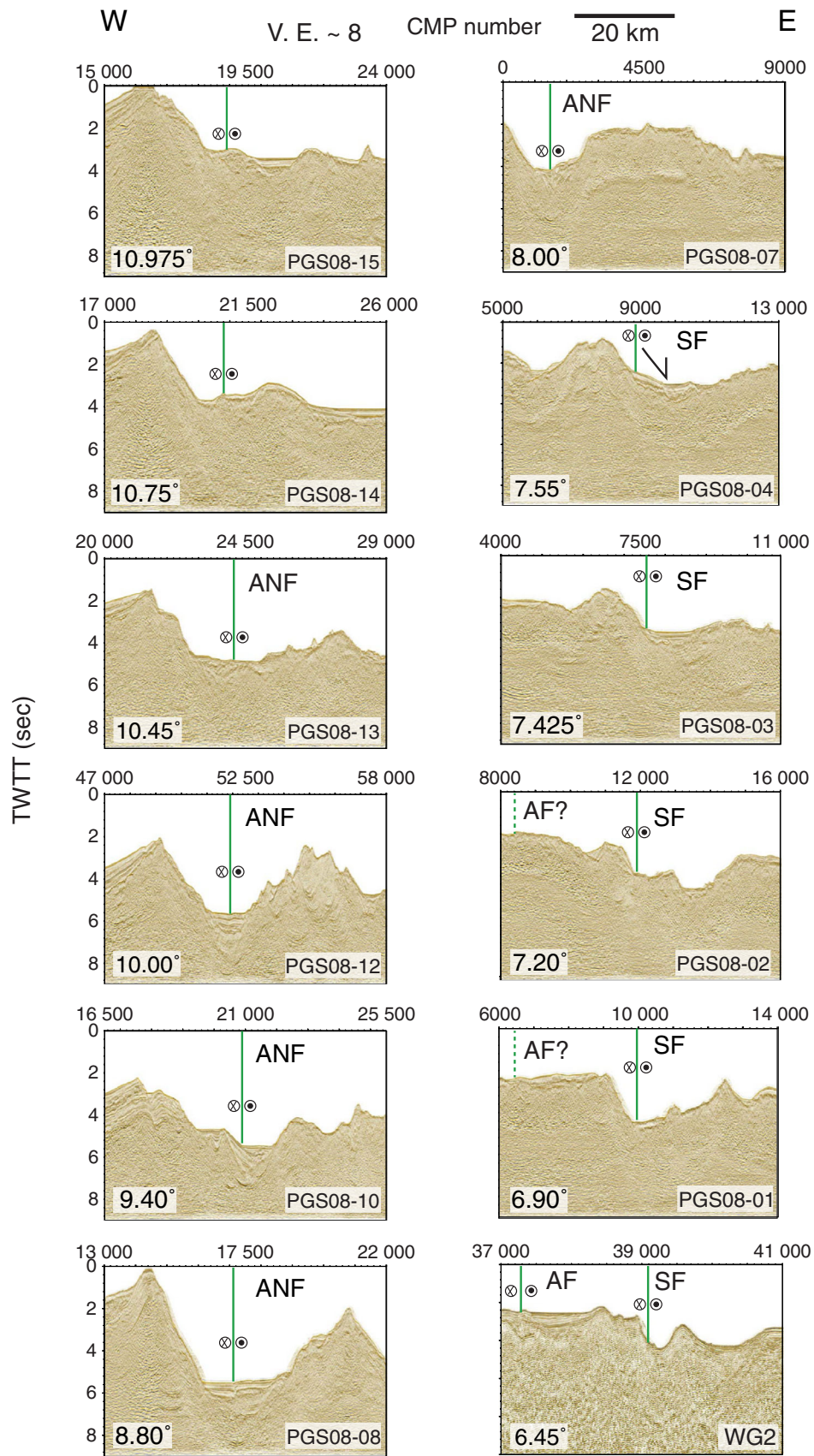
Figure 10. Seismic reflection images, from north to south, of the northward extension of the Great Sumatra Fault, which has been interpreted as Andaman-Nicobar Fault (ANF) north of Nicobar Island and the Aceh (AF) and Seulimeum Faults (SF) to the south. The green line marks the faults' surface arrivals.
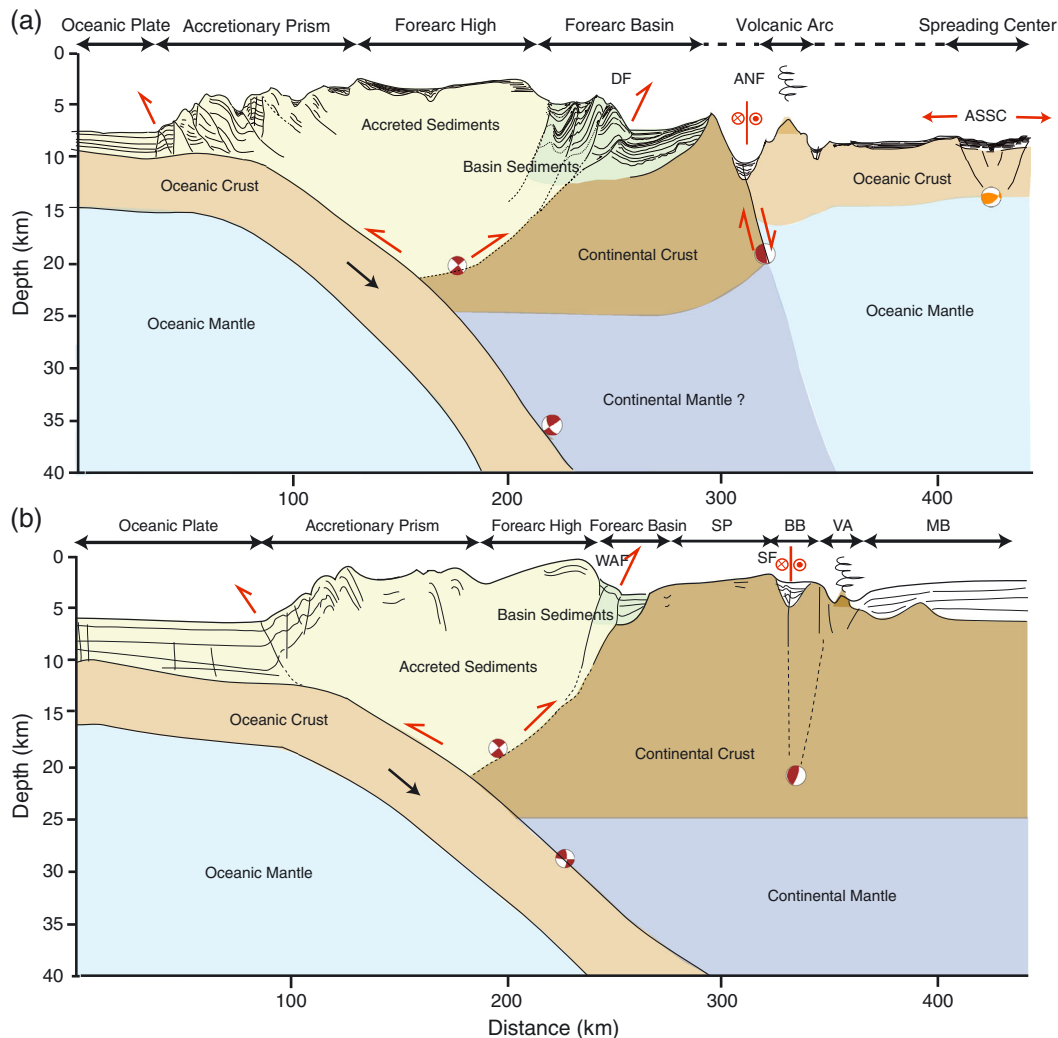
Figure 11. Summary sketch across the subduction zone from the oceanic plate to the back-arc basin down to 40 km depth (a) in the Andaman Sea (e.g., PGS08-12 to PGS08-15), and (b) off of northern Sumatra (e.g., WG2). Focal mechanisms are shown to illustrate the deformation and the orientation of the fault planes. DF: Diligent Fault, ANF: Andaman-Nicobar Fault, ASSC: Andaman Sea Spreading Center, WAF: West Andaman Fault, SF: Seulimeum Fault, BB: Breueh Basin, MB: Mergui Basin, SP: Sumatra Platform, VA: Volcanic Arc.

westernmost back thrust, at CMP 8700, seems to have created a piggyback basin, which lies beneath 500 ms thick flat lying sediments, with some deformation at the seafloor. A second small back thrust, at CMP 9100, shows some deformation on the seafloor. The most active (blind) back thrust is near CMP 10,000, dividing the fore-arc basin from the recent fore-arc high (Figures 7 and 9). Profile PGS08-14 is about 30 km south of profile PGS08-15 and also shows three back thrusts; the easternmost is most active and seems to arrive on the seafloor. There is a blind thrust within the fore-arc basin, deforming the sediments, suggesting that the back thrusts propagate eastward over time, similarly to what is observed in the Mentawai Basin [*Mukti et al.*, 2012]. Profile PGS08-13, which is 60 km farther south, has three very impressive back thrusts. The two westernmost are associated with very deep (2 s) piggyback basins and seem to be active. Profile PGS08-12 is 60 km farther south, and seems to have only one back thrust bounding the fore-arc basin with the present day

fore-arc high, which contains up to 2 s thick uplifted sediments. The lower sedimentary strata at the western end of the NAB are deformed, suggesting the presence of an ancient thrust system. Profile PGS08-11 contains two active back thrusts. Profile PGS08-10, which is ~60 km farther south of profile PGS08-11, contains several folded ridges; one inactive and one active back thrust can be easily observed. Profile PGS08-09 contains a very narrow 4 s thick deep basin, where sediments show very little deformation. This deep basin could either be a part of the fore-arc basin or formed by the presence of a strike-slip fault. This basin is bounded by ridges showing thrust type deformation, suggesting that this region has experienced transpressional deformation. This complex deformation continues farther south along profile PGS08-08, where five eastward (instead of westward) steeply dipping thrusts can be observed. The presence of thick deformed sediments suggests that the deformation is younger than the sediment deposition. Profiles PGS08-05 to PGS08-07, not shown in

Figure 8, do not show any sign of back thrusting as they are too close to the intersection of the strike-slip fault in the north with that in the south. On the other hand, the western part of profile PGS08-04 shows a back thrust with a narrow fore-arc basin, similar to that in profile WG2, where the fore-arc basin is wider. It is interesting to note that bottom-simulating reflectors are (BSRs) widely observed in the fore-arc basins and within the back thrusted area of our profiles, but they are absent from the deformation front all along the margin.

5.7. Sliver Fault (Andaman-Nicobar Fault)

[36] Figure 10 shows seismic profiles that cross the sliver strike-slip fault, the Andaman-Nicobar Fault (ANF), from north to south. On profiles PGS08-14 and PGS08-15, the strike-slip fault is expressed as a small compressional ridge with a flower structure, similar to what is seen along profile WG2 for the Aceh Fault. The ANF lies in a deep basin, bounded in the west by a steep marginal fault and in the east by a sedimented ridge. These two profiles are north of the intersection of the strike-slip sliver fault and the ASSC. The presence of only a few strike-slip earthquakes with complex fault plane solutions in this region (Figure 2) is consistent with limited transpressional deformation suggested by seismic images. Profile PGS08-13 is close to the intersection of the ASSC and the ANF, where the strike-slip deformation is expressed by a V-shaped sedimentary basin with a complex deformation pattern. A clear strike-slip fault with a vertical slip of 50 m is imaged in the center of the deep basin on profile PGS08-12, as discussed above. On profile PGS08-10, the expression of the sliver strike-slip fault becomes complex again, and it is difficult to pinpoint the precise location of the fault, as it looks more like a ~20 km wide zone of deformation. On the other hand, the strike-slip sliver fault is imaged like a knife-edge on profile PGS08-08, which is 120 km farther south, similar to that on profile PGS08-12. On profile PGS08-07, which is located 150 km farther south, a clear fault is imaged with a vertical offset of 150 m, along with some complex deformation pattern. The large cluster of earthquakes after the 2004 great Sumatra earthquake occurred in this region. The focal mechanisms of the earthquakes further confirm the complex deformation pattern (Figures 2 and 5). It should also be noted that the distribution of hypocenters is not vertical as one would expect from strike-slip faulting, but it has a slight tilt toward northeast, which can also be observed on profile PGS08-07. This lithospheric-scale eastward dip on the sliver strike-slip fault might explain the westward tilting of the whole fore-arc basin system and the presence of the EMF. Profile PGS08-04 is south of the intersection of the ANF, SF, and WAF. It contains a push-up ridge and normal fault in the center of the basin; therefore, it is difficult to define the precise location of the strike-slip fault, but these structures could be controlled by a strike-slip fault at depth. There is no clear evidence of a strike-slip fault on profile PGS08-03, but a subsiding basin is present, which is underlain by thick eastward tilted sediments, suggesting a deep rooted strike-slip fault. Profile PGS08-02 has two eastward steeply dipping normal faults, defining a stair-cased basin, with a tilted fault block in the center, suggesting the presence of a rift system. The central tilted block has some undeformed sediments whereas the basin floors do not have much sediment and are likely to be of volcanic origin. Profile PGS08-01 has only a large eastward

dipping normal fault with a volcano at the center, similar to profile WG2. We define the location of the Seulimeum Fault (SF) as a large step in bathymetry. It also contains some deformed sediments on the SW side, which may represent the passage of the Aceh fault.

5.8. Summary of Interpretations

[37] Fore-arc highs lie all along the Andaman-Sumatra margin and are expressed as a chain of islands and shallow ridges. On the seaward side, they are bounded by a series of trenchward vergent thrust faults. On the fore-arc basin side, the margin is complex but northeastward or eastward verging (westward dipping) back thrusts are observed along all the profiles (Figure 9). The fore-arc basins are underlain by continental crust with the thickest sediments in the northeast or east of the back thrusts. The root of the back thrusts lies at the contact between the continental crust and the accretionary wedge, which acts as a backstop [*Singh et al.*, 2012; *Mukti et al.*, 2012]. *Mukti et al.* [2012] suggested that there might be some 85 Ma old sediments at the base of the fore-arc basins, which might be relevant for oil and gas exploration.

[38] The sliver GSF traverses mainland Sumatra and is enveloped by the volcanoes along the volcanic arc, but there seems to be no direct link between the two [*Sieh and Natawidjaja*, 2000]. The GSF is well separated from the back thrust bounding the fore-arc basin. Just north of Sumatra, the sliver strike-slip fault and volcanic arc are joined by a rift basin, the Weh Basin, but are separated from the back thrust and fore-arc basin by the Sumatra Continental Platform (Figure 10), the width of which diminishes around Nicobar Island, bringing all the above systems very close to each other, and hence making their interpretation very difficult. Farther north of Nicobar Island, the distance between the back thrusts and sliver strike-slip fault increases due to the presence of the fore-arc basin, and the volcanic arc lies just east of the strike-slip fault (Figure 11). The fore-arc basin between Nicobar and Andaman, which we named the Nicobar Andaman Basin (NAB) (Figure 7), is similar to the fore-arc basin observed in the Mentawai region (Figure 8). Since the fore-arc basin in the Mentawai region is underlain by continental crust, we suggest that the NAB is also underlain by continental crust. The similarity between the steep faults and narrow deep basins south (Weh) and north of Nicobar Island suggests that they are of the same origin. Since the Weh basin is formed by the rifting of the continental crust, we suggest that the steep fault north of Nicobar Island, which we have called the Andaman-Nicobar Fault, defines a rifted margin of the continental crust from the Malaya peninsula. The sliver strike-slip fault, the ANF, lies in the rifted valley, which has some dip-slip component. Previous authors [e.g., *Curray*, 2005; *Cochran*, 2010] have defined this fault as the northward continuation of the WAF. As we shall see in the next section, the WAF is a back thrust and so is the DF. We thus redefine this section of the sliver strike-slip fault as the Andaman-Nicobar Fault (ANF). The volcanic arc lies farther east of this fault. At around 10°N, the ANF connects the Sagaing fault in Myanmar through the spreading center and the transform fault in the central Andaman Sea.

6. Discussion

[39] Here we focus our discussion on the back thrust, the sliver strike-slip faults, and the rift basins, and discuss how

our results complement previous observations and deepen our understanding of the dynamics in the Andaman Sea.

6.1. Back Thrust

[40] The WAF in the Andaman Sea was previously interpreted as the strike-slip sliver fault, defining the eastern boundary of the fore-arc basin based on bathymetry, and as the boundary between the Burma and Sunda plates south of the ASSC [e.g., *Curray*, 2005; *Cochran*, 2010]. South of 7° N, the WAF has also been interpreted as a strike-slip fault [*Singh*, 2005; *Sibuet et al.*, 2007; *Seeber et al.*, 2007; *Berglar et al.*, 2010]. Based on deep seismic reflection and refraction studies, *Singh et al.* [2012] suggested that it is a back thrust. Similarly, the Mentawai Fault system is also proven to consist of a set of back thrusts [*Mukti et al.*, 2012], which get younger toward the fore-arc basin. Farther northward, the Diligent Fault, which also consists of set of back thrusts, marks the western boundary of the fore-arc basin (Figures 7 and 9). Therefore, we conclude that the Diligent Fault is similar to the WAF south of Nicobar Island, and corresponds to a system of back thrusts, although the southern portion of this fault seems to contain some complex deformation, including some strike-slip component. The presence of steeply dipping (~30°) thrust earthquakes around profile PGS08-12 indicates that some of the faults are active. The DF was first characterized as primarily a normal fault that may also have experienced strike-slip motion [*Curray*, 2005]. This view was later contradicted by *Cochran* [2010] who suggested the DF is a compressional feature resulting from the deformation of the hanging wall of the EMF, but our results clearly show that the DF is a back thrust, similar to the WAF and Mentawai Fault zone offshore southern Sumatra. Our seismic coverage is up to 11°N. However, the combined bathymetry and gravity data suggest that back thrusting can be extended up to 12°N (Figure 2), but the structure farther north looks more complex as was observed along profiles PGS08-08 and PGS08-09.

[41] The DF, as a continuation of the WAF and the Mentawai Fault offshore western Sumatra, explains the presence of the chain of islands on one side and the fore-arc basin on the other side where the back thrust is responsible for the uplift of the islands. The back thrust also defines the boundary between the continental crust and the accretionary wedge, and acts as a thrust over a backstop. Back thrusting and seaward dipping back stops have also been observed in other active accretionary wedges such as the Mediterranean ridge [*Le Pichon et al.*, 1982] and Lesser Antilles [*Westbrook et al.*, 1988; *Biju-Duval et al.*, 1982; *Byrne et al.*, 1993]. Our conclusion of the extensive back thrusting all along Andaman-Sumatra margin is consistent with the mechanical modeling of a doubly convergent margin [*Willet et al.*, 1993].

[42] The EMF (Figure 5) shows normal components and seems to be less active. It might result from large-scale westward tilting of the fore-arc basin system and might define the western boundary of the rifted Sunda continental crust at depth. *Cochran* [2010] had also traced the EMF from 8°30′N to 11°00′N and interpreted it as a down-to-the-east normal fault, corresponding to the western edge of the fore-arc gravity low and suggested that sediment packages thickening toward the center of the basin indicated continuing subsidence and motion along the EMF. Although some motion is accommodated along the EMF, it is the least active fault in the region.

6.2. Sliver Strike-Slip Fault

[43] The GSF constitutes the sliver fault on mainland Sumatra [*Sieh and Natawidjaja*, 2000] and divides into two strands as it enters the Andaman Sea: the Aceh fault in the west and the Seulimeum fault in the east. *Ghosal et al.* [2012] have found that the Aceh strand is the most seismically active branch, contradicting the results of *Sieh and Natawidjaja* [2000] who concluded that the Aceh strand is presently inactive. Previous workers [e.g., *Curray*, 2005; *Cochran*, 2010] had interpreted the WAF as the strike-slip sliver fault but, as we have shown, the WAF, as well as the DF to the north, are back thrusts. The two strike-slip and back thrust systems merge east of Nicobar Island and then separate again. We image the northward extension of the Great Sumatra fault in the Andaman Sea as the Andaman-Nicobar fault (ANF) from 8°00′N to the ASSC (Figure 10), which we interpret as the sliver plate fault accommodating the trench-parallel component of motion, and defining the sliver plate boundary in the Andaman Sea.

[44] The distance between the subduction front and the sliver strike-slip fault is 275 km along profile CGGV010, and decreases to 250 km near Nias Island, 225 km along profile WG2, and 175 km along profile PGS08-06. This distance increases again to 250 km along profile PGS08-12. Where the distance to the trench is minimum, just east of Nicobar Island, there is a change in the direction of the sliver fault from N150E to NS. The obliquity does not seem to have much effect on the position of the strike-slip fault. *Molnar and Dayem* [2010] suggested that the position of intracontinental strike-slip faults is defined by a zone of weakness, a discontinuity in strength of the lithosphere, where the strain concentrates along the boundary between weak and strong lithosphere. In the case of the GSF on mainland Sumatra, the fault passes in the vicinity of the volcanic arc, which would create a zone of weakness at depth, separating the fore arc from the back arc. North of Banda Aceh, the zone of weakness is created by rifting along the SF. North of Nicobar Island, the continental fore-arc crust in the west is separated by oceanic crust in the east. The situation is similar farther north along the Sagaing Fault, as well as along the Denali and Fairweather Faults in North America, Philippine Fault, and Alpine Fault in New Zealand [*Molnar and Dayem*, 2010].

[45] On the other hand, the along-strike trend in distance between the subduction front and back thrust is complicated. It increases from 120 km north of Siberut Island to 170 in Southern Sumatra. It is ~140 km along profile WG2, 125 km around profile PGS08-02, increases to 230 km along profile PGS08-09, and then decreases to 185 km along profile PGS0815. It seems the location of the back thrust is controlled by the presence of the continental backstop and the complexity on the lower plate. Indeed, the shortest distance (120 km) between the subduction front and the back thrust is where the Investigator and the Ninety East Ridges indent the subduction front.

[46] As noted previously, the 2004 great Sumatra earthquake ruptured 1300 km of the plate boundary from north of Banda Aceh all the way to the northern tip of Andaman Island. This pure thrust event in oblique subduction setting is likely to have induced stress on the Aceh Fault and ANF; indeed *McCloskey et al.* [2005] and *Cattin et al.* [2009] have shown that the stress has changed along these faults and that they could be site of

great damaging earthquakes. Although a large number of earthquakes have occurred on the ANF (Figure 2), the 200 km segment of the Aceh Fault has remained silence for a long time and hence could produce a large earthquake in the near future.

6.3. Rift System

[47] Rift basins are observed on all the profiles from 5°N to 12°N. These basins along profiles WG2 and PGS08-01 and PGS08-02 seem to be due to the rifting of the continental crust as the area around them is of continental origin, whereas the area around the rift basins imaged on profiles PGS08-03 and PGS08-04 could be either of continental or volcanic origin. As we have discussed above, the western margin of the rift basin along profiles PGS08-07 to PGS08-15 is of continental origin. The relatively high gravity anomaly on the eastern side of the fore-arc high on profile PGS08-06 suggests the presence the continental crust there. Therefore, it is possible that the whole of the southwestern and western side of the deep rift basin, from 5°N to 14°N, is bounded by continental crust: the Sumatra continental crust in the south, and the Malaya continental crust north of 7°N. South of 7°N, the northeastern side of the rift basin is likely bounded by the continental crust or a fragment of continental crust as the volcanic arc lies within the rift basin, whereas north of 7°N, the volcanic arc and oceanic crust bound the basin.

[48] The rifting could be due to a combination of pull-apart process along sliver strike-slip faults and back-arc extension (spreading). The whole continental block beneath the fore-arc basin, including the Invisible Bank (Figure 11) that forms the western shoulder of the rift basin, seems to have significantly tilted westward due to a large eastward slip (up to 4 km) along a normal fault responsible for creating the rift basin. *Kamesh Raju et al.* [2004] have suggested that the Andaman Sea spreading has propagated westward toward the ANF. The position of the rifting in the Andaman Sea has changed several times in the last 40 Ma [*Curray*, 2005], and the present day rift basins might reflect this change. The transition from the shallow fore arc to the deeper back-arc region is the result of opening/rifting in the Andaman Sea, where faults only act as a secondary process, rather than to subduction erosion as *Cochran* [2010] had proposed.

7. Conclusions

[49] Combined seismic reflection, bathymetry, gravity, and earthquake data from offshore Andaman-Nicobar have allowed us to define several important features that are consistent with observations offshore central Sumatra. The following conclusions are drawn from this study:

[50] 1. We find that the West Andaman and the Diligent Faults, defining the boundary between the fore-arc high and the fore-arc basin, are predominantly back thrusts and correspond to the Mentawai back thrust system observed in the Mentawai region farther south.

[51] 2. The Nicobar Andaman fore-arc basin is floored by the Malaya continental crust and belongs to the same regime as the floor of the Mentawai basin farther south. The oldest sediments could be up to 85 Ma old. The Invisible Bank seems to be of continental origin and bounds a deep rift basin, and might have rifted from the Malaya Peninsula about 23–30 Ma ago during the initiation of spreading in the Andaman Sea.

[52] 3. A deep rift basin is observed all along of our profiles from 5°N to 14°N. It seems to be active from offshore Banda Aceh all the way to the junction of the Andaman-Nicobar Fault and the Andaman Sea Spreading Centre. South of 7°N, it hosts the volcanic arc whereas north of 7°N, it hosts the Andaman-Nicobar Fault.

[53] 4. The GSF seems to branch into two strands as it enters the sea in the north: the Aceh Fault and the Seulimeum fault. The Aceh fault is the main strike-slip fault, whereas the Seulimeum fault bounds the rift system until 7°N. North of 7°N, the Andaman-Nicobar Fault is the main strike-slip fault and acts as a sliver fault up to 10°N when it encounters the Andaman Sea Spreading Centre. Hence, the GSF and ANF are the main sliver strike-slip fault.

[54] 5. The volcanic arc lies within the rift basin south of 7°N whereas it lies east of the basin north of 7°N.

References

Abercrombie, R. E., M. Antolik, and G. Ekström (2003), The June 2000 M_w 7.9 earthquake south of Sumatra: Deformation in the India-Australia plate, *J. Geophys. Res.*, *410*(B1), 2018, doi:10.1029/2001JB000674.

Berglar, K., C. Gaedicke, D. Franke, S. Ladage, K. Klingelhoefer, and Y. S. Djajadihardja (2010), Structural evolution and strike-slip tectonics off north-western Sumatra, *Tectonophysics*, *480*, 119–132.

Biju-Duval, B., B. P. Le Quellec, A. Mascle, V. Renard, and P. Valey (1982), Multibeam bathymetric survey and high resolution seismic investigations on the Barbados ridge complex (eastern Caribbean): A key to the knowledge and interpretation of an accretionary wedge, *Tectonophysics*, *86*, 275–304.

Briggs, R. W., et al. (2006), Deformation and slip along the Sunda Megathrust in the great 2005 Nias-Simeulue earthquake, *Science*, *311*, 1897–1901.

Byrne, D., W. Wang, and D. M. Davis (1993), Mechanical role of backstops in the growth of forearcs, *Tectonics*, *12*, 123–144.

Cameron, N. R., H. Ngabito, K. S. Miswar, and H. H. Syah (1980). The geological evolution of northern Sumatra, in Indonesian Petroleum Association, Proceedings of the 9th Annual Convention, Jakarta, 9, 149–187.

Cattin, R., N. Chamot-Rooke, M. Pubellier, A. Rabaute, M. Delescluse, C. Vigny, L. Fleitout, and P. Dubernet (2009), Stress change and effective friction coefficient along the Sumatra-Anadman-Sagaing fault system after the 26 December 2004 ($Mw = 9.2$) and the 28 March ($Mw = 8.7$) earthquakes, *Geochem. Geophys. Geosyst.*, *10*, Q03011, doi:10.1029/2008GC002167.

Chauhan, A. P. S., S. C. Singh, N. D. Hananto, H. Carton, F. Klingelhoefer, J.-X. Dessa, H. Permana, N. J. White, D. Graindorge, and SumatraOBS Scientific Team (2009), Seismic imaging of forearc backthrusts at northern Sumatra subduction zone, *Geophys. J. Int.*, *179*, 1772–1780.

Chlieh, M., et al. (2007), Coseismic slip and aftershock of the great *Mw* 9.15 Sumatra-Andaman earthquake of 2004, *Bull. Seismol. Soc. Am.*, *97*, S152–S173, doi:10.1785/0120050631.

Cochran, J. (2010), Morphology and tectonics of the Andaman Forearc, northeastern Indian Ocean, *Geophys. J. Int.*, *182*, 613–651.

Crow, M. J. (2005), Tertiary volcanicity, in *Sumatra Geology, Resources and Tectonic Evolution*, edited by A. J. Barber, M. J. Crow, and J. S. Milsom, pp. 98–119, The Geological Society, London.

Curray, J. R. (2005), Tectonics and history of Andaman Sea region, *J. Asian Earth Sci.*, *25*, 187–232.

Curray, J. R., D. G. Moore, L. A. Lawver, F. J. Emmel, R. W. Raitt, M. Henry, and R. Kieckhefer (1979), Tectonics of Andaman Sea and Burma, in *Geological and Geophysical Investigations of Continental Margins*, edited by J. S. Watkins, L. Montadert, and P. W. Dickerson, pp. 189–198, Amer. Assoc. Petrol. Geol. Memoir 29, Tulsa, Okla.

Delescluse, M., N. Chamot-Rooke, R. Cattin, L. Fleitout, O. Trubienko, and C. Vigny (2012), April 2012 intra-oceanic seismicity off Sumatra boosted by the Banda-Aceh megathrust, *Nature*, *490*, 240–244, doi:10.1038/nature11520.

Deplus, C. (2001), Indian Ocean actively deforms, *Science*, *292*, 1850–1851.

Deplus, C., M. Diament, H. Hébert, G. Bertrand, S. Dominguez, J. Dubois, J. Malod, P. Patriat, B. Pontoise, and J.-J. Sibilla (1998), Direct evidence of active deformation in the eastern Indian oceanic plate, *Geology*, *26*, 131–134.

Diament, M., H. Harjono, K. Karta, C. Deplus, D. Dahrin, M. T. Zen Jr., M. Gérard, O. Lassal, A. Martin, and J. Malod (1992), Mentawai fault zone off Sumatra—A new key to the geodynamics of western Indonesia, *Geology*, 20, 259–262.

Duputel, Z., H. Kanamori, V. Tsai, L. Rivera, L. Meng, J.-P. Ampuero, and J. Stock (2012), The 2012 Sumatra great earthquake sequence, *Earth Planet. Sci. Lett.*, 351–352, 247–257, doi:10.1016/j.epsl.2012.07.017.

Engdahl, E. R., A. Villasenor, H. R. DeShon, and C. H. Thurber (2007), Teleseismic relocation and assessment of seismicity (1918–2005) in the region of the 2004 M_w 9.0 Sumatra-Andaman and 2005 M_w 8.6 Nias Island great earthquakes, *Bull. Seismol. Soc. Am.*, 97, S43–S61.

Fitch, T. J. (1972), Plate convergence, transcurrent faults, and initial deformation adjacent to southeast Asia and the western Pacific, *J. Geophys. Res.*, 77, 4432–4460.

Fujii, Y., and K. Satake (2007), Tsunami source of the 2004 Sumatra-Andaman earthquake inferred from tide gauge and satellite data, *Bull. Seismol. Soc. Am.*, 97(1A), S192–S207.

Gahalaut, V. K., B. Nagarajan, J. K. Catherine, and S. Kumar (2006), Constraints on 2004 Sumatra-Andaman earthquake rupture from GPS measurements in Andaman-Nicobar Islands, *Earth Planet. Sci. Lett.*, 242, 365–374.

Ghosal, D., S. C. Singh, A. P. S. Chauhan, and N. Hananto (2012), New insights on the offshore extension of the Great Sumatran fault, NW Sumatra, from marine geophysical studies, *Geochem. Geophys. Geosyst.*, 13, Q0AF06, doi:10.1029/2012GC004122.

Kamesh Raju, K. A., T. Ramprasad, P. S. Rao, B. Ramalingeswara Rao, and J. Varghese (2004), New insights into the tectonic evolution of the Andaman basin, northeast Indian Ocean, *Earth Planet. Sci. Lett.*, 221, 145–162.

Kamesh Raju, K. A., D. Ray, A. Mudholkar, G. P. S. Murty, V. K. Gahalaut, K. Samudrala, A. L. Paropkari, R. Ramachandran, and L. S. Prakash (2012), Tectonic and volcanic implications of a cratered seamount off Nicobar Island, Andaman Sea, *J. Asian Earth Sci.*, 56, 42–53.

Katili, J. (1973), Geochronology of West Indonesia and its implication on plate tectonics, *Tectonophysics*, 19, 195–212.

Katili, J. A. (1975), Volcanism and plate tectonics in the Indonesian island arcs, *Tectonophysics*, 26, 165–188.

Klootwijk, C. T., J. S. Gee, J. W. Pierce, and G. M. Smith (1992), Neogene evolution of the Himalayan Tibetan region – constraints from ODP site 758, northern Ninetyeast Ridge- bearing on climatic change, *Paleogeogr. Paleoclimatol. Paleoecol.*, 95, 95–110.

Konca, A. O., et al. (2008), Partial rupture of a locked patch of the Sumatra megathrust during the 2007 earthquake sequence, *Nature*, 456, 631–635.

Kundu, B., D. Legrand, K. Gahalaut, V. K. Gahalaut, P. Mahesh, K. A. Kamesh Raju, J. K. Catherine, A. Ambikapthy, and R. K. Chadha (2012), The 2005 volcano-tectonic earthquake swarm in the Andaman Sea: Triggered by the 2004 great Sumatra-Andaman earthquake, *Tectonics*, 31, TC5009, doi:10.1029/2012TC003138.

Lay, T., et al. (2005), The Great Sumatra-Andaman Earthquake of 26 December 2004, *Science*, 308, 1127–1133.

Le Pichon, X., N. Lyberis, J. Angelier, and V. Renard (1982), Strain distribution over the Mediterranean Ridge a synthesis incorporating new Sea-Beam data, *Tectonophysics*, 86, 243–274.

McCaffrey, R. (1992), Oblique plate convergence, slip vectors, and forearc deformation, *J. Geophys. Res.*, 97, 8905–8915.

McCaffrey, R. (2009), The tectonic framework of the Sumatra subduction zone, *Annual Rev Earth. Planet Sci.*, 37, 345–66.

McCloskey, J., S. S. Nalbant, and S. Stacey (2005), Earthquake risk from co-seismic stress, *Nature*, 434, 291.

Molnar, P., and C. E. Dayem (2010), Major intracontinental strike-slip faults and contrasts in lithospheric strength, *Geosphere*, 6, 444–467.

Mukti, M. M., S. C. Singh, I. Deighton, N. Hananto, R. Moeremans, and H. Permana (2012), Structural evolution of backthrusting in the Mentawai Fault Zone, offshore Sumatran forearc, *Geochem. Geophys. Geosyst.*, 13, Q12006, doi:10.1029/2012GC004199.

Paul, J., et al. (2001), The motion and active deformation of India, *Geophys. Res. Lett.*, 28, 647–650.

Peltzer, G., and P. Tapponnier (1988), Formation and evolution of strike-slip faults, rifts and basins during the India-Asia collision: an experimental approach, *J. Geophys. Res.*, 93, 15,085–15,097.

Pesicek, J. D., C. H. Thurber, H. Zhang, H. R. DeShon, E. R. Engdahl, and S. Widiyantoro (2010), Teleseismic double-difference relocation of earthquakes along the Sumatra-Andaman subduction zone using a 3-D model, *J. Geophys. Res.*, 115, B10303, doi:10.1029/2010JB007443.

Rhie, J., D. Dreger, R. Bürgmann, and B. Romanowicz (2007), Slip of the 2004 Sumatra–Andaman earthquake from joint inversion of long-period global seismic waveforms and GPS static offsets, *Bull. Seismol. Soc. Am.*, 97(1A), S115–S127.

Rock, N. M. S., H. H. Syah, A. E. Davis, D. Hutchison, M. T. Styles, and R. Lena (1982), Permian to recent volcanism in Northern Sumatra, Indonesia: A Preliminary study of its distribution, chemistry, and peculiarities, *Bull. Volcanol.*, 45–2, 127–152.

Roy, T. K., and N. N. Chopra (1987), Wrench faulting in Andaman forearc basin, India, *Proc. Annu. Offshore Technol. Conf.*, 19, 393–404.

Sandwell, D. T., and W. H. F. Smith (2009), Global marine gravity from retracked Geosat and ERS-1 altimetry: Ridge segmentation versus spreading rate, *J. Geophys. Res.*, 114, B01411, doi:10.1029/2008JB006008.

Seeber, L., C. Mueller, T. Fujiwara, K. Aria, W. Soh, Y. S. Djajadihardja, and M. H. Cormier (2007), Accretion, mass wasting, partitioning strain over the 26th December 2004 Mw 9.2 rupture offshore Aceh, northern Sumatra, *Earth Planet Sci. Lett.*, 263, 16–31.

Sevilgen, V., R. S. Stein, and F. F. Pollitz (2012), Stress imparted by the great 2004 Sumatra earthquake shut down transforms and activated rifts up to 400 km away in the Andaman Sea, *Proc. Natl. Acad. Sci. U.S.A.*, 109, 15,152–15,156, doi:10.1073/pnas.1208799109.

Sibuet, J.-C., et al. (2007), 26th December 2004 Great Sumatra-Andaman Earthquake: Co-seismic and post-seismic motions in northern Sumatra, *Earth Planet. Sci. Lett.*, 263, 88–103.

Sieh, K., and D. Natawidjaja (2000), Neotectonic of the Sumatran fault Indonesia, *J. Geophys. Res.*, 105, 28,295–28,326.

Singh, S. C. (2005), Sumatra earthquake research indicates why rupture propagated northward, *Eos Trans. AGU*, 86, 497–502.

Singh, S. C., et al. (2008), Seismic evidences for broken oceanic crust in the 2004 Sumatra earthquake epicentral region, *Nat. Geosci.*, 1(11), 771–781.

Singh, S. C., H. Hananto, A. P. S. Chauhan, H. Permana, M. Denolle, A. Hendriyana, and D. Natawidjaja (2010), Seismic evidence of active backthrusting at the NE Margin of Mentawai Islands, SW Sumatra, *Geophys. J. Int.*, 180, 703–714.

Singh, S. C., N. Hananto, and A. Chauhan (2011a), Enhanced reflectivity of backthrusts in the recent great Sumatran earthquake rupture zones, *Geophys. Res. Lett.*, 38, L04302, doi:10.1029/2010GL046227.

Singh, S. C., et al. (2011b), Aseismic zone and earthquake segmentation associated with a deep subducted seamount in Sumatra, *Nat. Geosci.*, 4, 308–311.

Singh, S. C., A. P. S. Chauhan, A. J. Calvert, N. D. Hananto, D. Ghosal, A. Rai, and H. Carton (2012), Seismic evidence of bending and unbending of subducting oceanic crust and the presence of mantle megathrust in the 2004 Great earthquake rupture zone, *Earth Planet. Sci. Lett.*, 321–322, 166–176.

Subarya, C., M. Chlieh, L. Prawirodirdjo, J. P. Avouac, Y. Bock, K. Sieh, A. J. Meltzner, D. H. Natawidjaja, and R. McCaffrey (2006), Plate-boundary deformation associated with the great Sumatra–Andaman earthquake, *Nature*, 440, 46–51, doi:10.1038/nature04522.

Westbrook, G. K., J. W. Ladd, P. Buhl, N. Bangs, and G. J. Tiley (1988), Cross section of an accretionary wedge: Barbados Ridge complex, *Geology*, 16, 631–635.

Willet, S., C. Beaumont, and P. Fullssack (1993), Mechanical model for the tectonics of doubly vergence compressional orogens, *Geology*, 21, 371–374.